

This is an Accepted Manuscript of an article published by Elsevier in *Insect Biochemistry and Molecular Biology* on 12 Mar 2018, available online: <https://doi.org/10.1016/j.ibmb.2018.03.003>.

TITLE

A polydnavirus-encoded ANK protein has a negative impact on steroidogenesis and development

Authors and Affiliations

**Marilena Ignesti ^a, Rosalba Ferrara ^b, Patrizia Romani ^{a,c}, Luca Valzania ^{a,d},
Giulia Serafini ^a, Francesco Pennacchio ^{b,*}, Valeria Cavaliere ^{a,**}, Giuseppe
Gargiulo ^{a,***}**

^a Dipartimento di Farmacia e Biotecnologie, Università di Bologna, Via Selmi 3
Bologna, Italy.

^b Dipartimento di Agraria – Laboratorio di Entomologia “E. Tremblay”, Università di
Napoli ‘Federico II’, Portici (NA), Italy.

^c Present address: Dipartimento di Medicina Molecolare, Università di Padova,
Padova, Italy.

^d Present address: Department of Entomology, University of Georgia, Athens, GA
30602, USA.

* Corresponding author. Dipartimento di Agraria – Laboratorio di Entomologia “E.
Tremblay”, Università di Napoli ‘Federico II’, Portici (NA), Italy.

** Corresponding author. Dipartimento di Farmacia e Biotecnologie, Università di
Bologna, Via Selmi 3 Bologna, Italy.

*** Corresponding author. Dipartimento di Farmacia e Biotecnologie, Università di
Bologna, Via Selmi 3 Bologna, Italy.

Abstract

Polydnaviruses (PDV) are viral symbionts associated with ichneumonid and braconid wasps parasitizing moth larvae, which are able to disrupt the host immune response and development, as well as a number of other physiological pathways. The immunosuppressive role of PDV has been more intensely investigated, while very little is known about the PDV-encoded factors disrupting host development. Here we address this research issue by further expanding the functional analysis of *ankyrin* genes encoded by the bracovirus associated with *Toxoneuron nigriceps* (Hymenoptera, Braconidae). In a previous study, using *Drosophila melanogaster* as experimental model system, we demonstrated the negative impact of *TnBVank1* impairing the ecdysone biosynthesis by altering endocytic traffic in prothoracic gland cells. With a similar approach here we demonstrate that another member of the viral *ank* gene family, *TnBVank3*, does also contribute to the disruption of ecdysone biosynthesis, but with a completely different mechanism. We show that its expression in *Drosophila* prothoracic gland (PG) blocks the larval-pupal transition by impairing the expression of steroidogenic genes. Furthermore, we found that *TnBVank3* affects the expression of genes involved in the insulin/TOR signaling and the constitutive activation of the insulin pathway in the PG rescues the pupariation impairment. Collectively, our data demonstrate that *TnBVANK3* acts as a virulence factor by exerting a synergistic and non-overlapping function with *TnBVANK1* to disrupt the ecdysone biosynthesis.

Keywords

Bracovirus; Drosophila; ANK proteins; Ecdysone biosynthesis; insulin/TOR signaling

1 **1. Introduction**

2 Parasitic wasps develop on a wealth of insect species, on which they induce a number
3 of physiological and developmental alterations, which are essential to create a suitable
4 environment for the development of their progeny (Pennacchio and Strand, 2006).

5 These changes are currently denoted as host regulation, which is a complex process
6 mediated by a network of molecular interactions, triggered and controlled by factors
7 produced and released into the host by the ovipositing females (i.e. venom, microbial
8 symbionts, ovarian secretions) and/or by the embryo (i.e. teratocytes, cells deriving
9 from the dissociation of the embryonic membrane) or larvae (Pennacchio and Strand,
10 2006). Among microbial symbionts, polydnviruses (PDVs) are potent

11 immunosuppressive agents associated with ichneumonid and braconoid wasps
12 parasitizing larval stages of moth larvae, and able to induce a number of pathological
13 alterations in the host (Pennacchio and Strand, 2006; Strand and Burke, 2015). PDVs
14 are integrated as proviruses in the wasp genome and replicate only in the epithelial
15 cells of the ovarian calyx to produce free virions that are injected into the host at the
16 oviposition. During this process they infect and express virulence factors in several
17 host tissues, without undergoing replication (Herniou et al., 2013; Strand and Burke,
18 2015). The segmented genome of PDVs consists of multiple circles of DNA of
19 different size, characterized by large non-coding segments and by genes showing an
20 eukaryotic structure, often organized in gene families (Herniou et al., 2013; Strand
21 and Burke, 2015). One of the most widespread gene family encodes ankyrin motif
22 proteins (ANK), which are virtually expressed in all host tissues and found associated
23 with a number of different pathological symptoms, ranging from immune to
24 developmental alterations (Falabella et al., 2007; Strand and Burke, 2013). The viral
25 ANK proteins have sequence similarity with members of I κ B protein family, which

26 control the NF- κ B signaling in insects and vertebrate innate immunity (Silverman and
27 Maniatis, 2001). Due to the lack of the regulatory sequences needed for their signal-
28 induced and basal degradation, these ANK proteins appear to irreversibly bind to host
29 NF- κ B factors and block their transcriptional activity. Therefore, a function as
30 suppressors of the host immune system has been proposed and demonstrated for some
31 members of PDV *ank* genes (Thoetkiattikul et al., 2005; Falabella et al., 2007; Bitra et
32 al., 2012). In contrast, we know comparatively much less on the role of *ank* genes,
33 and more in general of PDV-encoded factors, in the induction of host developmental
34 alterations.

35 The host-parasitoid association *Heliothis virescens-Toxoneuron nigriceps*
36 (Lepidoptera, Noctuidae - Hymenoptera, Braconidae) provides a valuable
37 experimental model system to study the molecular bases of developmental arrest of
38 mature larvae, which is due to a combined action of PDV and teratocytes, disrupting
39 the biosynthetic activity of prothoracic glands (Pennacchio et al., 1997, 1998) and the
40 ecdysteroid metabolism (Pennacchio et al., 1994a) respectively. Since the ecdysone
41 biosynthesis is well conserved in insects (Niwa and Niwa, 2014), to identify whether
42 *TnBV* genes can disrupt this biosynthetic pathway, we took advantage of the
43 *Drosophila melanogaster* model system that allow to design experiments that are not
44 doable in *Heliothis*. The powerful molecular genetics techniques that can be applied
45 in *Drosophila* (del Valle Rodriguez et al., 2011) allow the study of the effect that the
46 expression of virulence genes has on specific tissues during development. Indeed, this
47 model system has been even employed for studying human viral pathogens (Hughes
48 et al., 2012).

49 Using this approach, in our previous work, we have gained insights on the role of a
50 member of the viral *ank* gene family of *TnBV*, *TnBVank1* (Duchi et al., 2010;

51 Valzania et al., 2014). We found that it functions as a virulence gene disrupting
52 ecdysteroidogenesis in prothoracic gland by interfering with the endocytic trafficking
53 of steroidogenic cells (Valzania et al., 2014). *TnBV* genome carries two other
54 members of the *ank* gene family (Falabella et al., 2007). In the present study we
55 analyzed the effect of the expression of the *TnBVank3* in *Drosophila* steroidogenic
56 cells. We found that also this gene contributes to the disruption of ecdysone
57 biosynthesis by altering the expression of steroidogenic genes.

58

59 **2. Materials and methods**

60

61 *2.1. Fly strains*

62 Fly stocks were raised on standard cornmeal/yeast/agar medium at 18°C. *y w^{67c23}* was
63 used as the wild type stock in this study. We used the following Bloomington stocks:
64 #5138 (*y¹ w^{*}*; *P[tubP-Gal4]LL7/TM3, Sb¹ Ser¹*); #7019 (*w^{*}*; *P[w^{+mC}=tubP-*
65 *Gal80^{ts}]*20; *TM2/TM6B, Tb¹*); #8263 *y¹ w¹¹¹⁸*; *P[UAS-InR.A1325D]*2. *phm-Gal4*
66 (Ono et al., 2006) was a gift from C. Mirth (*phm-Gal4,UAS-mCD8::GFP/TM6B*).

67

68 *2.2. Crosses*

69 For the *tub-Gal80^{ts}*; *phm-Gal4* experiments, *tub-Gal80^{ts}*; *phm-Gal4/TM6B* females
70 were crossed at 21°C to *UAS-TnBVank3* males, or to *y w^{67c23}* males as control. Larvae
71 were raised at 21°C and transferred at 29°C at specific time points after egg laying
72 (AEL). For the *UAS-InR^{CA}* expression, *tub-Gal80^{ts}*; *phm-Gal4/TM6B* females were
73 crossed at 21°C to *UAS-InR^{CA}*; *UAS-TnBVank3* males, and to *UAS-InR^{CA}* males as
74 control. Larvae were raised at 21°C and transferred at 29°C after 3 days AEL.

75

76 2.3. *Generation of TnBVank3-HA-Myc transgenic line*

77 A construct containing the epitope tags hemagglutinin (*HA*) and *Myc* at the 3' end of
78 of *TnBVank3* gene was produced (Biomatik) and cloned into the pUAST-attb vector
79 (Bischof et al., 2007). The transgenic *Drosophila* line carrying the UAS-*TnBVank3*-
80 *HA-Myc* chimeric gene was obtained by phiC31 integrase-mediated insertion into the
81 attP2 landing-site locus on the third chromosome by BestGene Inc (USA).

82

83 2.4. *Immunofluorescence microscopy*

84 Immunostaining on ring glands was performed as described previously (Valzania et
85 al., 2016). The *TnBVANK3-HA-Myc* protein was detected using a polyclonal rabbit
86 anti-*HA* 1:50 (Santa Cruz Biotechnology, USA) and anti-rabbit Cy3-conjugated
87 1:2000 (Invitrogen, USA). The glands were mounted in Fluoromount G (Electron
88 Microscopy Sciences, USA) and analyzed with TCS SL Leica confocal system.
89 Images were processed using Adobe Photoshop CS6.

90

91 2.5 *Protein Extracts and Western Blot Analysis*

92 *UAS-TnBVank3-HA-Myc* or control *y w^{67c23}* males were crossed at 25 °C to *tub*-
93 *Gal4/TM3*. Third instar larvae were collected and the total protein extraction and blot
94 analysis were performed as already described (Romani et al., 2016). The *TnBVANK3*-
95 *HA-Myc* protein was detected using a monoclonal mouse anti-*HA* 1:100 (Santa Cruz
96 Biotechnology, USA) and ECL Plex anti-mouse Cy3 1:2500 (GE Healthcare, USA).

97

98 2.6. *20-E rescue experiments*

99 Two groups of ten *tub-Gal80^{ts}*; *phm-Gal4/ UAS-TnBVank3* larvae, initially raised at
100 21°C for 3 days AEL and then transferred at 29°C for other 3 days were collected and

101 placed in new tubes with yeast paste supplemented with 20-hydroxyecdysone (Sigma)
102 1 mg/ml and kept at 29°C. As a control the same experiments were carried out on
103 larvae of the same genotype fed with yeast paste containing an equal amount of
104 ethanol.

105

106 2.7. *Quantitative Real-Time PCR (qRT-PCR)*

107 For *E74A*, *E75A* and steroidogenic gene expression experiments, total RNA was
108 isolated from 3 independent biological samples of 5 larvae or prepupae. Total RNA
109 was isolated using TRIzol reagent (Thermo Scientific), and DNA was removed by
110 RNase-Free DNase Set (Ambion). qRT-PCR was performed on an ABI PRISM 7900
111 Real-Time PCR system (Applied Biosystems) by means of the Power SYBR-Green
112 RNA-to-Ct-1-Step Kit (Applied Biosystems).

113 For the expression analysis of insulin and TOR pathway components, 15 brain-ring
114 gland complexes (BRGCs) were dissected, in PBS buffer, from four independent
115 biological samples. Total RNA was isolated using TRIzol reagent (Thermo Scientific),
116 and contaminant DNA was removed by RNase-Free DNase Set (Ambion). cDNA
117 synthesis was carried out with dT-primed M-MLV Reverse Transcriptase
118 (LifeTechnologies). Quantitative PCR was carried out with FastStart SYBR Green
119 Master Mix (Roche) on a QuantStudio 6 real-time thermal cycler.

120 The qRT-PCR primers used are listed in Table S1 in the supplementary material. For
121 all of the genes examined, the reactions were conducted in technical triplicates. All
122 transcript expression values were normalized to *Rpl23* gene.

123

124 2.8. *Prothoracic gland size measurements*

125 For measurements of the PG area, confocal images of PGs taken at 40X magnification
126 were quantified with Photoshop CS6.

127

128 2.9. Statistical analysis

129 GraphPad Prism software was used for statistical analysis. Statistical significance was
130 determined on the basis of unpaired *t*-test performed on the means and *p* values were
131 calculated (*=*p*<0.05; **=*p*<0.01 and ***=*p*<0.001). *p*<0.05 was considered
132 statistically significant. All results are expressed as the mean ± standard deviation
133 (SD).

134

135 3. Results and Discussion

136 3.1. Expression of *TnBVank3* in the prothoracic gland induces developmental arrest 137 at third instar

138 *TnBVANK3* is 168 aa long and contains 3 ankyrin repeats (Fig. 1A). To test the effect
139 of the viral *TnBVANK3* protein on *Drosophila* development we used the GAL4/UAS
140 binary expression system (Brand and Perrimon, 1993). We produced *Drosophila*
141 transgenic lines carrying a UAS transgene encoding *TnBVANK3* protein tagged at the
142 C terminus with the hemagglutinin (HA) and c-Myc epitopes. The expression of the
143 *TnBVank3-HA-Myc* gene (hereafter abbreviated as *TnBVank3*) was assessed using the
144 ubiquitous *tubulin-Gal4* driver (*tub-Gal4*, hereafter abbreviated as *tub*>). The
145 *TnBVANK3* protein was detected in third instar *tub*>*TnBVank3* larvae by western
146 blot on whole cell lysate, using anti-HA antibody. A band in the size range of 23 kDa
147 was detected, as expected for the *TnBVANK3-HA-Myc* protein (Fig. 1B). No signal
148 was observed in protein extracts from the control larvae *tub*>+. The ubiquitous
149 expression of *TnBVank3* driven by the *tub*> driver did not affect larval development.

150 However, no *tub>TnBVank3* adult flies were obtained, since after pupariation the
151 pupae degenerate (data not shown). This phenotype suggested that *TnBVank3*
152 expression could affect metamorphosis, without any impact on larval molts, as
153 observed in host larvae parasitized by *T. nigriceps* (Pennacchio et al., 1994b). Pulses
154 of the hormone ecdysone (E) dictate the precise timing of the developmental
155 transitions in *Drosophila*, such as larval molts, pupariation and metamorphosis
156 (Warren et al., 2006). Ecdysone is synthesized in the steroidogenic cells of the
157 prothoracic gland (PG) and secreted into the hemolymph, to reach peripheral tissues
158 where it is converted to its active form, 20-hydroxyecdysone (20E). To test whether
159 *TnBVANK3* affects *Drosophila* development impairing the prothoracic gland
160 function, we specifically targeted the expression of *TnBVank3* in this gland using the
161 *phantom-Gal4* driver (*phm-Gal4*, hereafter abbreviated as *phm>*), which allows high
162 expression level of UAS transgene in the PG. We expressed *TnBVank3* in PG cells of
163 larvae, at specific time points after egg laying (AEL) using a temperature sensitive
164 form of the Gal4 repressor Gal80, Gal80^{ts} (McGuire et al., 2003), which allows
165 modulation of Gal4 activity. We used *tub-Gal80^{ts}; phm-Gal4 (Gal80^{ts}; phm>)* to
166 control the timing of *TnBVank3* expression in the PG cells. *Gal80^{ts}; phm>TnBVank3*
167 and control *Gal80^{ts}; phm>+* larvae were initially raised at 21°C, and at the early L2
168 stage (3 days AEL) were shifted to the restrictive temperature (29°C) to promote Gal4
169 activity. The temperature shift did not affect the normal development of control
170 individuals. Conversely, at 29°C the larvae expressing *TnBVank3* exhibited a fully
171 penetrant phenotype showing a block of larval-pupal transition, as observed in *H.*
172 *virescens* larvae parasitized by *T. nigriceps* (Pennacchio et al., 1994b). After 2 days
173 the *Gal80^{ts}; phm>TnBVank3* larvae are similar in size to control larvae (Fig. 2A).
174 However, at the third day, while control larvae pupate, *Gal80^{ts}; phm>TnBVank3* do

175 not. During their prolonged L3 larval life that extended up to 3-4 weeks, the *Gal80^{ts}*;
176 *phm>TnBVank3* larvae continue to increase in size (Fig. 2A). When the *Gal80^{ts}*;
177 *phm>TnBVank3* larvae are shifted from 21°C to 29°C at 4 days AEL, some of them
178 pupariated, while all the larvae shifted at 29°C, at 5 days AEL, regularly pupariated.
179 Thus, when *TnBVank3* expression is triggered in the PG cells of L2 larvae it causes
180 the block of pupariation.

181

182 3.2. *TnBVank3* affects ecdysone activity

183 At the end of larval development a high peak of ecdysone triggers pupariation. In our
184 experimental conditions (larvae initially raised at 21°C for 3 days AEL and then
185 shifted to 29°C) in wild type larvae pupariation occurs after 3 days at 29°C with the
186 formation of white prepupae. To investigate whether the block of the transition to
187 pupal stage caused by the expression of *TnBVank3* was due to a low level of 20E, we
188 carried out ecdysone-feeding rescue experiments. Third instar *Gal80^{ts}*;
189 *phm>TnBVank3* larvae after 3 days at 29°C were transferred to new vials containing
190 yeast paste supplemented with 20E dissolved in ethanol or just ethanol. After 24 h at
191 29°C all the larvae fed with 20E had developed into pupae (100%, *n*=20) (Fig. 2B).
192 Conversely, the *Gal80^{ts}*; *phm>TnBVank3* larvae fed with yeast and ethanol, as a
193 control, did not form any puparia and all of them persisted as third instar (*n*=20). This
194 result indicates that the expression of *TnBVank3* in the PG impairs the biosynthesis of
195 ecdysone. We therefore investigated the ecdysone activity by measuring the
196 expression levels of two 20E-inducible transcription factors, *E74A* and *E75A*, which
197 are required to undertake metamorphosis (Karim and Thummel, 1992) and can be
198 used as readout for ecdysone levels. We induced *TnBVank3* expression in PG of
199 larvae and, after 2 and 3 days at 29°C, we analyzed by qRT-PCR the expression levels

200 of *E74A* and *E75A* genes in *Gal80^{ts}*; *phm>TnBVank3* larvae and in *Gal80^{ts}*; *phm>+*
201 control larvae/white prepupae of the same age (Fig. 2C). The expression of both
202 *E74A* and *E75A* was significantly reduced in *TnBVank3* larvae (after 2 days at 29°C),
203 as well as in larvae after 3 days at 29°C compared to the control white prepupae.
204 Collectively these data indicate that in the *TnBVank3* larvae the ecdysone biosynthesis
205 is impaired causing the block of larval development.

206

207 3.3. *TnBVANK3* affects the expression of steroidogenic genes

208 Ecdysone is synthesized from cholesterol in the steroidogenic cells of the PG (Fig.
209 3A). Cholesterol, which cannot be synthesized by insects (Gilbert and Warren, 2005),
210 enters the steroidogenic cells through a receptor-mediated low-density lipoprotein
211 endocytic pathway (Rodenburg and Van der Horst, 2005), which delivers cholesterol
212 to the endosomes. A number of ecdysone biosynthetic genes have been identified and
213 characterized in *Drosophila* (Fig. 3A) (Gilbert and Warren, 2005; Niwa and Niwa,
214 2014). The first enzymatic reaction of the pathway, the conversion of cholesterol to 7-
215 dehydrocholesterol (7dC) is catalyzed by Neverland (Nvd) (Yoshiyama et al., 2006;
216 Yoshiyama-Yanagawa et al., 2011). 7dC is then converted to 5β-ketodiol (KD)
217 through the ‘Black Box’, a biosynthetic step not yet characterized, in which Shroud
218 (Sro), Spook (Spo) and Spookier (Spok) are involved (Namiki et al., 2005; Ono et al.,
219 2006, 2012; Niwa et al., 2010). Phantom (Phm) transforms KD in ketotriol (KT),
220 Disembodied (Dib) converts KT in 2-deoxyecdysone (2dE) and Shadow (Sad)
221 converts 2dE to ecdysone (E) (Chavez et al., 2000; Warren et al., 2002, 2004; Petryk
222 et al., 2003; Niwa et al., 2004). After release from the PG into the hemolymph, E is
223 converted in peripheral tissues to its active form 20-hydroxyecdysone (20E) by Shade
224 (Shd) enzyme (Petryk et al., 2003).

225 We investigated whether expression of steroidogenic genes was affected by
226 *TnBVank3* expression in the PG cells. We compared by qRT-PCR the expression
227 levels of *nvd*, *spok*, *sro*, *phm*, *dib* and *sad* genes in *Gal80^{ts}; phm>TnBVank3* larvae
228 kept of 2 and 3 days at 29°C with that in *Gal80^{ts}; phm>+* control larvae kept of 2
229 days at 29°C and white prepupae of 3 days at 29°C (Fig. 3B). Expression of
230 *TnBVank3* in the PG resulted in a down-regulation of steroidogenic genes, with a
231 more pronounced effect on *nvd*, *spok* and *sro*, which catalyze early steps in the
232 ecdysone biosynthetic pathway.

233 These data further support our finding that *TnBVANK3* impairs the ecdysone
234 biosynthesis.

235

236 3.4. *TnBVANK3* affects PG size

237 To investigate the *TnBVANK3* distribution in PG cells expressing the *TnBVank3*
238 gene, we performed immunostaining experiments using an anti-HA antibody on
239 *Gal80^{ts}; phm>TnBVank3* PGs of third instar larvae (after 2 days at 29°C).

240 Interestingly, *TnBVANK3* was localized only in the nucleus of PG cells (Fig. 4A,B).
241 Since, the *phm-Gal4* stock that we used carries the *UAS-mCD8::GFP* construct, the
242 detection of the mCD8::GFP cell membrane marker allowed us to visualize the PGs
243 (Fig. 4B). *TnBVank3* expression did not alter the gross morphology of the PG
244 (compare Videos S1 and S2), although the PG size was smaller than in control PGs
245 (-17.7% Fig. 4C), as observed also in parasitized tobacco budworm larvae
246 (Pennacchio et al., 1997).

247

248 3.5. *TnBVANK3* reduces the expression of the insulin/TOR signaling components

249 In *Drosophila*, as in the other holometabolous insects, metamorphosis can start after
250 the larvae have reached the appropriate size, known as critical weight (CW). In
251 *Drosophila* CW is attained in the early half of the L3 instar larvae. The achievement
252 of CW is associated with the activation of steroidogenesis, which is controlled by a
253 complex regulatory network of cross-modulating molecular events (Niwa and Niwa,
254 2016).

255 The prothoracicotropic hormone (PTTH) produced by the brain stimulates the
256 synthesis of ecdysone by targeting its receptor Torso in the PG cells, which influences
257 both the activation of ecdysone biosynthesis and CW control (McBrayer et al., 2007;
258 Rewitz et al., 2009). The insulin/TOR (target of rapamycin) signaling, which controls
259 growth rate and body size, do also promote growth of PG cells and their biosynthetic
260 activity (timing and amount) (Yamanaka et al., 2013), is part of the complex
261 molecular network assessing the CW and controlling the downstream developmental
262 events (Koyama et al., 2014). It has been shown that increasing insulin signaling in
263 the PG causes an increase of gland size and ecdysone biosynthesis, which results into
264 a precocious metamorphosis, leading to pupae and adults of reduced size (Caldwell et
265 al., 2005; Colombani et al., 2005; Mirth et al., 2005). Conversely, a down-regulation
266 of the insulin signaling has a negative impact on gland size and ecdysone
267 biosynthesis, which determines a delayed pupariation, giving rise to larger pupae and
268 adults. A more severe phenotype is produced in response to the knock down of TOR,
269 controlling the progression of PG endocycle required for activation of ecdysone
270 biosynthesis, which determines a reduction of PG size and a down-regulation of
271 ecdysteroidogenic genes associated with a developmental arrest of third instar larvae
272 (Ohhara et al., 2017)

273 The negative effect of *TnBVank3* on the ecdysone biosynthesis and the PG size,
274 coupled with a severe developmental arrest phenotype, produced when this gene is
275 expressed from the L2 stage, before the CW is reached, suggested that *TnBVANK3*
276 impairs the insulin/TOR signaling. To test this hypothesis, we investigated the mRNA
277 levels of the insulin/TOR signaling components in the BRGCs of *Gal80^{ts}*;
278 *phm>TnBVank3* and *Gal80^{ts}* ; *phm>+* control larvae kept for 2 days at 29°C. For the
279 insulin pathway we found a significant reduced expression of *InR*, *Pi3K* and *Akt* genes
280 (Fig. 5A). The analysis of the TOR pathway also revealed a significant decrease of the
281 mRNA levels of *Tor* and the key downstream effector *S6 kinase (S6k)* (Fig. 5A).
282 We next investigated whether the activation of InR pathway could rescue the
283 pupariation defect induced by *TnBVANK3*. We found that the expression in the PG
284 cells of a constitutively active form of the insulin receptor (*InR^{CA}*) was able to restore
285 pupariation (Fig. 5B). Accordingly to the constitutive activation of insulin pathway,
286 the control larva expressing only *InR^{CA}* advanced the onset of metamorphosis giving
287 rise to small pupae (Caldwell et al., 2005; Colombani et al., 2005). This phenotype
288 was also produced in the *InR^{CA}; TnBVank3* larvae.

289 Collectively, our data suggest that in the *TnBVank3* larvae the reduction of
290 insulin/TOR signaling contributes to the negative effect on ecdysone biosynthesis.
291 Although our findings indicate that a reduction of the expression of steroidogenic
292 genes underlies the *TnBVANK3* developmental arrest phenotype, we cannot assert
293 that this down-regulation is only due to the reduction of insulin/TOR signaling or
294 whether *TnBVANK3* might also act directly on disrupting biosynthetic enzyme gene
295 expression. However, if and how *TnBVANK3* may have an impact on other
296 transduction pathways controlling steroidogenesis remains to be studied.

297 **4. Conclusions**

298 Our study on the viral *ank* gene *TnBVank3* clearly points out its role in blocking
299 ecdysone biosynthesis. A similar effect was produced by the expression of another
300 member of the same gene family, *TnBVank1* (Valzania et al., 2014). Interestingly,
301 these two genes target different parts of the ecdysone biosynthetic pathway, while
302 *TnBVANK3* localizes into the nucleus and causes a reduced expression of
303 steroidogenic genes, *TnBVANK1* acts in the cytoplasm, by blocking the cholesterol
304 trafficking. The high similarity of natural host phenotypes induced by the PDV
305 infection with those we produced in the *Drosophila* model system, by expressing
306 specific PDV genes, paves the way for further experiments on the natural host, aiming
307 to shed light if the complementary and synergistic effects of these two virulence
308 factors are adopted by parasitic wasps to ensure a complete block of host ecdysone
309 biosynthesis and its larval development.

310

311 **Figure captions**

312 **Fig. 1.** Inducible expression of *TnBVANK3*-HA-Myc chimeric protein.

313 (A) Scheme showing the amino acid sequence of *TnBVANK3* and the HA and Myc
314 epitopes fused at its carboxy terminus. The underlined Ankyrin repeat domains were
315 predicted by searching the sequences using the SMART database (Simple Modular
316 Architecture Research Tool; <http://smart.embl-heidelberg.de/>), using the default
317 parameters (Schultz et al., 1998). (B) Western blot of third instar larvae cell lysate
318 using anti-HA antibody. Larvae expressing the *UAS-TnBVank3-HA-Myc* transgene by
319 the ubiquitous driver *tub-Gal4* show a band in the size range of 23 kDa that
320 corresponds to the predicted *TnBVANK3*-HA-Myc protein. This band is absent in
321 control larvae *tub>+* carrying only the Gal4 driver.

322

323 **Fig. 2.** *TnBVank3* expression in the PG cells affects the ecdysone biosynthesis
324 causing the block of the transition from larval to pupal stage.
325 (A) Light micrographs of *Gal80^{ts}; phm>TnBVank3* and *Gal80^{ts}; phm>+* larvae of
326 different ages at 29°C. (B) Rescue experiments of *Gal80^{ts}; phm>TnBVank3* with 20-
327 hydroxyecdysone (20E). After 3 days at 29°C *Gal80^{ts}; phm>TnBVank3* larvae fed
328 with medium supplemented with 20E induces the pupariation (red), while larvae fed
329 with medium containing ethanol (EtOH) do not pupate (green). (C) qRT-PCR
330 analyses of the mRNA levels of the 20E-inducible transcriptional factors (*E74A*,
331 *E75A*) of *Gal80^{ts}; phm>+* and *Gal80^{ts}; phm>TnBVank3* of individuals kept at 29°C
332 for the indicated days. Graphs represent mean \pm SD; $n=3$; $**=p<0.01$; $***=p<0.001$.
333

334 **Fig. 3.** *TnBVANK3* reduces the expression of genes of the ecdysone biosynthetic
335 pathway. (A) Scheme showing the steps in the conversion of cholesterol to ecdysone
336 (E). (B) qRT-PCR analysis of the transcript levels of the ecdysone biosynthetic
337 enzymes of individuals of the reported genotypes kept at 29°C for the indicated days.
338 Graphs represent mean \pm SD; $n=3$; $*=p<0.05$; $**=p<0.01$; $***=p<0.001$.
339

340 **Fig. 4.** *TnBVANK3* localization in the PG cells and its effects on PG size.
341 (A,B) Immunolocalization of *TnBVANK3*-HA-Myc with anti-HA antibody (red) in
342 PG cells of third instar *Gal80^{ts}; phm>TnBVank3* larvae (marked with mCD8::GFP,
343 green, B). *TnBVANK3* shows a nuclear localization. (C) The *Gal80^{ts};*
344 *phm>TnBVank3* PGs are significantly smaller (-17.7%) than PGs from control
345 *Gal80^{ts}; phm>+* larvae. The graph represents the mean \pm SD; 16 *Gal80^{ts};*
346 *phm>TnBVank3* PGs and 10 *Gal80^{ts}; phm>+* PGs analyzed; $**=p<0.01$.

347 **Fig. 5.** *TnBVANK3* affects the expression of the insulin/TOR signaling components.
348 (A) qRT-PCR analysis of the transcript levels of *InR*, *Pi3K*, *Akt*, *Tor* and *S6k* in the
349 BRGC of the control and *TnBVank3* larvae that were raised at 21°C for 3 days AEL
350 and then kept at 29°C for 2 days. Graphs represent mean \pm SD; $n=4$; $*=p<0.05$;
351 $**=p<0.01$; $***=p<0.001$. (B) Coexpression in the PGs of *TnBVank3* and the
352 constitutively active form of insulin receptor (*InR^{CA}*). Activation of insulin signaling
353 restores pupariation in *TnBVank3* larvae. The described results were obtained by
354 analyzing larvae raised at 21°C for 3 days AEL and then were shifted to the 29°C
355 restrictive temperature.

356

357 **Video captions**

358

359 **Video S1**

360 Morphology of a PG gland expressing *TnBVank3* and the cell membrane marker

361 mCD8::GFP.

362 QuickTime movie of 50 confocal optical z stack sections each with a scan step size of

363 0.33 μm through the entire PG. The detection of the mCD8::GFP protein allow to

364 visualize the PG morphology.

365

366 **Video S2**

367 Morphology of a PG gland expressing the cell membrane marker mCD8::GFP.

368 QuickTime movie of 41 confocal optical z stack sections each with a scan step size of

369 0.33 μm through the entire PG. The detection of the mCD8::GFP protein allow to

370 visualize the PG morphology.

371

372 **Acknowledgements**

373 We thank Christen Mirth and Bloomington Stock Center for fly stocks. We thank
374 Davide Andrenacci for helpful suggestions and critical reading of the manuscript.
375 The work was supported by a research grant from University of Bologna (RFO 2014)
376 to GG and VC; by the project POR Campania FESR 2007-2013 Bio Industrial
377 Processes-BIP, and the project Safe & Smart (Cluster Agroalimentare Nazionale -
378 CTN01_00230_248064) to FP.

379

380 **Authors' contribution**

381 VC, GG and FP conceived the research. MI, PR, LV and GS performed *Drosophila*
382 experimental work and morphological analyses. RF and PR performed qRT-PCR
383 analyses. MI conceived and designed part of the experiments. VC, FP and GG wrote
384 the manuscript.

385

386 **REFERENCES**

387 Bischof, J., Maeda, R.K., Hediger, M., Karch, F., Basler, K., 2007. An optimized
388 transgenesis system for *Drosophila* using germ-line-specific phiC31 integrases. *Proc*
389 *Natl Acad Sci U S A* 104, 3312-3317.
390 Bitra, K., Suderman, R.J., Strand, M.R., 2012. Polydnavirus Ank proteins bind NF-
391 kappaB homodimers and inhibit processing of Relish. *PLoS Pathog* 8, e1002722.
392 Brand, A.H., Perrimon, N., 1993. Targeted gene expression as a means of altering cell
393 fates and generating dominant phenotypes. *Development* 118, 401-415.
394 Caldwell, P.E., Walkiewicz, M., Stern, M., 2005. Ras activity in the *Drosophila*
395 prothoracic gland regulates body size and developmental rate via ecdysone release.
396 *Curr Biol* 15, 1785-1795.
397 Chavez, V.M., Marques, G., Delbecque, J.P., Kobayashi, K., Hollingsworth, M., Burr,
398 J., Natzle, J.E., O'Connor, M.B., 2000. The *Drosophila* disembodied gene controls
399 late embryonic morphogenesis and codes for a cytochrome P450 enzyme that
400 regulates embryonic ecdysone levels. *Development* 127, 4115-4126.
401 Colombani, J., Bianchini, L., Layalle, S., Pondeville, E., Dauphin-Villemant, C.,
402 Antoniewski, C., Carre, C., Noselli, S., Leopold, P., 2005. Antagonistic actions of
403 ecdysone and insulins determine final size in *Drosophila*. *Science* 310, 667-670.
404 del Valle Rodriguez, A., Didiano, D., Desplan, C., 2011. Power tools for gene
405 expression and clonal analysis in *Drosophila*. *Nat Methods* 9, 47-55.

406 Duchi, S., Cavaliere, V., Fagnocchi, L., Grimaldi, M.R., Falabella, P., Graziani, F.,
407 Gigliotti, S., Pennacchio, F., Gargiulo, G., 2010. The impact on microtubule network
408 of a bracovirus IkappaB-like protein. *Cell Mol Life Sci* 67, 1699-1712.
409 Falabella, P., Varricchio, P., Provost, B., Espagne, E., Ferrarese, R., Grimaldi, A., de
410 Eguileor, M., Fimiani, G., Ursini, M.V., Malva, C., Drezen, J.M., Pennacchio, F.,
411 2007. Characterization of the IkappaB-like gene family in polydnviruses associated
412 with wasps belonging to different Braconid subfamilies. *J Gen Virol* 88, 92-104.
413 Gilbert, L.I., Warren, J.T., 2005. A molecular genetic approach to the biosynthesis of
414 the insect steroid molting hormone. *Vitam Horm* 73, 31-57.
415 Herniou, E.A., Huguet, E., Theze, J., Bezier, A., Periquet, G., Drezen, J.M., 2013.
416 When parasitic wasps hijacked viruses: genomic and functional evolution of
417 polydnviruses. *Philos Trans R Soc Lond B Biol Sci* 368, 20130051.
418 Hughes, T.T., Allen, A.L., Bardin, J.E., Christian, M.N., Daimon, K., Dozier, K.D.,
419 Hansen, C.L., Holcomb, L.M., Ahlander, J., 2012. *Drosophila* as a genetic model for
420 studying pathogenic human viruses. *Virology* 423, 1-5.
421 Karim, F.D., Thummel, C.S., 1992. Temporal coordination of regulatory gene
422 expression by the steroid hormone ecdysone. *EMBO J* 11, 4083-4093.
423 Koyama, T., Rodrigues, M.A., Athanasiadis, A., Shingleton, A.W., Mirth, C.K., 2014.
424 Nutritional control of body size through FoxO-Ultraspiracle mediated ecdysone
425 biosynthesis. *Elife* 3.
426 McBrayer, Z., Ono, H., Shimell, M., Parvy, J.P., Beckstead, R.B., Warren, J.T.,
427 Thummel, C.S., Dauphin-Villemant, C., Gilbert, L.I., O'Connor, M.B., 2007.
428 Prothoracicotropic hormone regulates developmental timing and body size in
429 *Drosophila*. *Dev Cell* 13, 857-871.
430 McGuire, S.E., Le, P.T., Osborn, A.J., Matsumoto, K., Davis, R.L., 2003.
431 Spatiotemporal rescue of memory dysfunction in *Drosophila*. *Science* 302, 1765-
432 1768.
433 Mirth, C., Truman, J.W., Riddiford, L.M., 2005. The role of the prothoracic gland in
434 determining critical weight for metamorphosis in *Drosophila melanogaster*. *Curr Biol*
435 15, 1796-1807.
436 Namiki, T., Niwa, R., Sakudoh, T., Shirai, K., Takeuchi, H., Kataoka, H., 2005.
437 Cytochrome P450 CYP307A1/Spook: a regulator for ecdysone synthesis in insects.
438 *Biochem Biophys Res Commun* 337, 367-374.
439 Niwa, R., Matsuda, T., Yoshiyama, T., Namiki, T., Mita, K., Fujimoto, Y., Kataoka,
440 H., 2004. CYP306A1, a cytochrome P450 enzyme, is essential for ecdysteroid
441 biosynthesis in the prothoracic glands of *Bombyx* and *Drosophila*. *J Biol Chem* 279,
442 35942-35949.
443 Niwa, R., Namiki, T., Ito, K., Shimada-Niwa, Y., Kiuchi, M., Kawaoka, S.,
444 Kayukawa, T., Banno, Y., Fujimoto, Y., Shigenobu, S., Kobayashi, S., Shimada, T.,
445 Katsuma, S., Shinoda, T., 2010. Non-molting glossy/shroud encodes a short-chain
446 dehydrogenase/reductase that functions in the 'Black Box' of the ecdysteroid
447 biosynthesis pathway. *Development* 137, 1991-1999.
448 Niwa, R., Niwa, Y.S., 2014. Enzymes for ecdysteroid biosynthesis: their biological
449 functions in insects and beyond. *Biosci Biotechnol Biochem* 78, 1283-1292.
450 Niwa, Y.S., Niwa, R., 2016. Transcriptional regulation of insect steroid hormone
451 biosynthesis and its role in controlling timing of molting and metamorphosis. *Dev*
452 *Growth Differ* 58, 94-105.
453 Ohhara, Y., Kobayashi, S., Yamanaka, N., 2017. Nutrient-Dependent Endocycling in
454 Steroidogenic Tissue Dictates Timing of Metamorphosis in *Drosophila melanogaster*.
455 *PLoS Genet* 13, e1006583.

456 Ono, H., Morita, S., Asakura, I., Nishida, R., 2012. Conversion of 3-oxo steroids into
457 ecdysteroids triggers molting and expression of 20E-inducible genes in *Drosophila*
458 *melanogaster*. *Biochem Biophys Res Commun* 421, 561-566.

459 Ono, H., Rewitz, K.F., Shinoda, T., Itoyama, K., Petryk, A., Rybczynski, R., Jarcho,
460 M., Warren, J.T., Marques, G., Shimell, M.J., Gilbert, L.I., O'Connor, M.B., 2006.
461 Spook and Spookier code for stage-specific components of the ecdysone biosynthetic
462 pathway in Diptera. *Dev Biol* 298, 555-570.

463 Pennacchio, F., Bradleigh Vinson, S., Tremblay, E., Ostuni, A., 1994a. Alteration of
464 ecdysone metabolism in *Heliothis virescens* (F.) (Lepidoptera: Noctuidae) larvae
465 induced by *Cardiochiles nigriceps* Viereck (Hymenoptera: Braconidae) teratocytes.
466 *Insect Biochemistry and Molecular Biology* 24, 383-394.

467 Pennacchio, F., Falabella, P., Sordetti, R., Paola, V., Malva, C., Bradleigh Vinson, S.,
468 1998. Prothoracic gland inactivation in *Heliothis virescens* (F.)
469 (Lepidoptera:Noctuidae) larvae parasitized by *Cardiochiles nigriceps* Viereck
470 (Hymenoptera: Braconidae). *Journal of Insect Physiology* 44, 845-857.

471 Pennacchio, F., Sordetti, R., Falabella, P., Vinson, S.B., 1997. Biochemical and
472 ultrastructural alterations in prothoracic glands of *Heliothis virescens* (F.)
473 (Lepidoptera: Noctuidae) last instar larvae parasitized by *Cardiochiles nigriceps*
474 Viereck (Hymenoptera: Braconidae). *Insect Biochemistry and Molecular Biology* 27,
475 439-450.

476 Pennacchio, F., Strand, M.R., 2006. Evolution of developmental strategies in parasitic
477 hymenoptera. *Annu Rev Entomol* 51, 233-258.

478 Pennacchio, F., Vinson, S.B., Tremblay, E., Tanaka, T., 1994b. Biochemical and
479 developmental alterations of *Heliothis virescens* (F.) (lepidoptera, noctuidae) larvae
480 induced by the endophagous parasitoid *Cardiochiles nigriceps viereck* (Hymenoptera,
481 braconidae). *Archives of Insect Biochemistry and Physiology* 26, 211-233.

482 Petryk, A., Warren, J.T., Marques, G., Jarcho, M.P., Gilbert, L.I., Kahler, J., Parvy,
483 J.P., Li, Y., Dauphin-Villemant, C., O'Connor, M.B., 2003. Shade is the *Drosophila*
484 P450 enzyme that mediates the hydroxylation of ecdysone to the steroid insect
485 molting hormone 20-hydroxyecdysone. *Proc Natl Acad Sci U S A* 100, 13773-13778.

486 Rewitz, K.F., Yamanaka, N., Gilbert, L.I., O'Connor, M.B., 2009. The insect
487 neuropeptide PTH activates receptor tyrosine kinase torso to initiate metamorphosis.
488 *Science* 326, 1403-1405.

489 Rodenburg, K.W., Van der Horst, D.J., 2005. Lipoprotein-mediated lipid transport in
490 insects: analogy to the mammalian lipid carrier system and novel concepts for the
491 functioning of LDL receptor family members. *Biochim Biophys Acta* 1736, 10-29.

492 Romani, P., Papi, A., Igesti, M., Soccolini, G., Hsu, T., Gargiulo, G., Spisni, E.,
493 Cavaliere, V., 2016. Dynamin controls extracellular level of Awd/Nme1 metastasis
494 suppressor protein. *Naunyn Schmiedebergs Arch Pharmacol* 389, 1171-1182.

495 Schultz, J., Milpetz, F., Bork, P., Ponting, C.P., 1998. SMART, a simple modular
496 architecture research tool: identification of signaling domains. *Proc Natl Acad Sci U S*
497 *A* 95, 5857-5864.

498 Silverman, N., Maniatis, T., 2001. NF-kappaB signaling pathways in mammalian and
499 insect innate immunity. *Genes Dev* 15, 2321-2342.

500 Strand, M.R., Burke, G.R., 2013. Polydnavirus-wasp associations: evolution, genome
501 organization, and function. *Curr Opin Virol* 3, 587-594.

502 Strand, M.R., Burke, G.R., 2015. Polydnaviruses: From discovery to current insights.
503 *Virology* 479-480, 393-402.

504 Thoetkiattikul, H., Beck, M.H., Strand, M.R., 2005. Inhibitor kappaB-like proteins
505 from a polydnavirus inhibit NF-kappaB activation and suppress the insect immune
506 response. *Proc Natl Acad Sci U S A* 102, 11426-11431.

507 Valzania, L., Ono, H., Ignesti, M., Cavaliere, V., Bernardi, F., Gamberi, C., Lasko, P.,
508 Gargiulo, G., 2016. *Drosophila* 4EHP is essential for the larval-pupal transition and
509 required in the prothoracic gland for ecdysone biosynthesis. *Dev Biol* 410, 14-23.

510 Valzania, L., Romani, P., Tian, L., Li, S., Cavaliere, V., Pennacchio, F., Gargiulo, G.,
511 2014. A polydnavirus ANK protein acts as virulence factor by disrupting the function
512 of prothoracic gland steroidogenic cells. *PLoS One* 9, e95104.

513 Warren, J.T., Petryk, A., Marques, G., Jarcho, M., Parvy, J.P., Dauphin-Villemant, C.,
514 O'Connor, M.B., Gilbert, L.I., 2002. Molecular and biochemical characterization of
515 two P450 enzymes in the ecdysteroidogenic pathway of *Drosophila melanogaster*.
516 *Proc Natl Acad Sci U S A* 99, 11043-11048.

517 Warren, J.T., Petryk, A., Marques, G., Parvy, J.P., Shinoda, T., Itoyama, K.,
518 Kobayashi, J., Jarcho, M., Li, Y., O'Connor, M.B., Dauphin-Villemant, C., Gilbert,
519 L.I., 2004. Phantom encodes the 25-hydroxylase of *Drosophila melanogaster* and
520 *Bombyx mori*: a P450 enzyme critical in ecdysone biosynthesis. *Insect Biochem Mol*
521 *Biol* 34, 991-1010.

522 Warren, J.T., Yerushalmi, Y., Shimell, M.J., O'Connor, M.B., Restifo, L.L., Gilbert,
523 L.I., 2006. Discrete pulses of molting hormone, 20-hydroxyecdysone, during late
524 larval development of *Drosophila melanogaster*: correlations with changes in gene
525 activity. *Dev Dyn* 235, 315-326.

526 Yamanaka, N., Rewitz, K.F., O'Connor, M.B., 2013. Ecdysone control of
527 developmental transitions: lessons from *Drosophila* research. *Annu Rev Entomol* 58,
528 497-516.

529 Yoshiyama, T., Namiki, T., Mita, K., Kataoka, H., Niwa, R., 2006. Neverland is an
530 evolutionally conserved Rieske-domain protein that is essential for ecdysone
531 synthesis and insect growth. *Development* 133, 2565-2574.

532 Yoshiyama-Yanagawa, T., Enya, S., Shimada-Niwa, Y., Yaguchi, S., Haramoto, Y.,
533 Matsuya, T., Shiomi, K., Sasakura, Y., Takahashi, S., Asashima, M., Kataoka, H.,
534 Niwa, R., 2011. The conserved Rieske oxygenase DAF-36/Neverland is a novel
535 cholesterol-metabolizing enzyme. *J Biol Chem* 286, 25756-25762.

Table S1. The primers used for qRT-PCR experiments

Gene	Forward	Reverse
<i>nvd</i>	5'-ACCTCCCCCTTATCCAAATG-3'	5'-AGCAACGCTTCCACCAATAC-3'
<i>sro</i>	5'-ATGAGCGGCAGTCAACTTCT-3'	5'-CAGGAAATCACGGTCATGTG-3'
<i>spok</i>	5'-TATCTCTTGGGCACACTCGCTG-3'	5'-GCCGAGCTAAATTTCTCCGCTT-3'
<i>phm</i>	5'-TCGTCGTGGGCGATTATTTTA-3'	5'-AAGGCCACTGGGTCCATGT-3'
<i>dib</i>	5'-TGCCCTCAATCCCTATCTGGTC-3'	5'-ACAGGGTCTTCACACCCATCTC-3'
<i>sad</i>	5'-AAGGAGCGAGCTACCAATGA-3'	5'-GCTGCTCAAAGTGTGATGGA-3'
<i>E74A</i>	5'-GCCCTTTATCGACGATGCAC-3'	5'-GCTCCATTCAGTTCGTTGCC-3'
<i>E75A</i>	5'-ACGATATCAGCAGGCCAATC-3'	5'-GAATGCACGCCGTAATGGAAAC-3'
<i>Rpl23</i>	5'-GCTCAGGAAGAAGGTCATGC-3'	5'-GGCTATAGAGCTTGCATTGGA-3'
<i>Akt</i>	5'-GCCAGATCATGACCGTCGAT-3'	5'-GTCATAGCCACCTCACCCAC-3'
<i>InR</i>	5'-TTCTCTGGGAAATGGCCACC-3'	5'-TCGCCGAAGACCTATGATGC-3'
<i>Pi3K</i>	5'-GCCAGAACTGTCCTCCGAAA-3'	5'-CTTCGCTGAATTTGCTCGG-3'
<i>Tor</i>	5'-GCTATGACGAGGCGAATGGA-3'	5'-TCTTGGGGAACAGCGTCTTC-3'
<i>S6k</i>	5'-GCCAGGAGACCATACAGCTC-3'	5'-TGCCATAACCACCTTTGCCA-3'

Figure 1

A

MMASNYSLNDFFKMYSRYGHNYFHHVCCWGNYKLLCVARPFIDLSNSHLLLEDV
DYQGMSCIHLAVICNPKNAREILQVLISWGVNINRQDEVTGESILHLAIKFHHLKL
TKWIIKYSGINLNIRNYNDESPYELAYKLNYYVMWLLRKNGAICEYRLTSSEES
SSED **HA** **Myc**

B

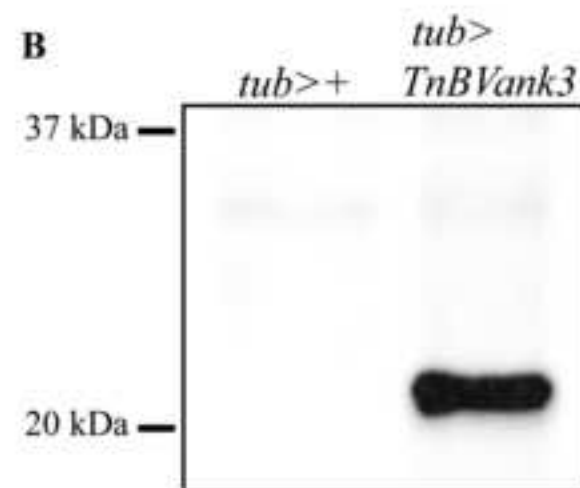


Figure 2

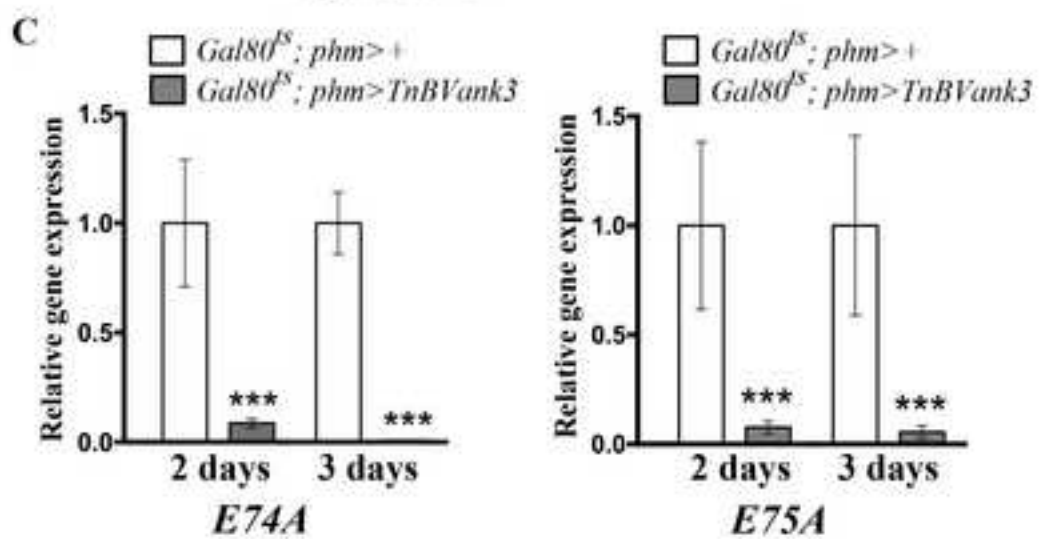
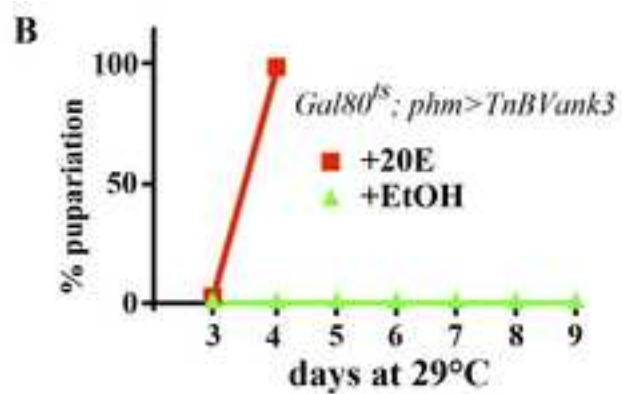


Figure 3

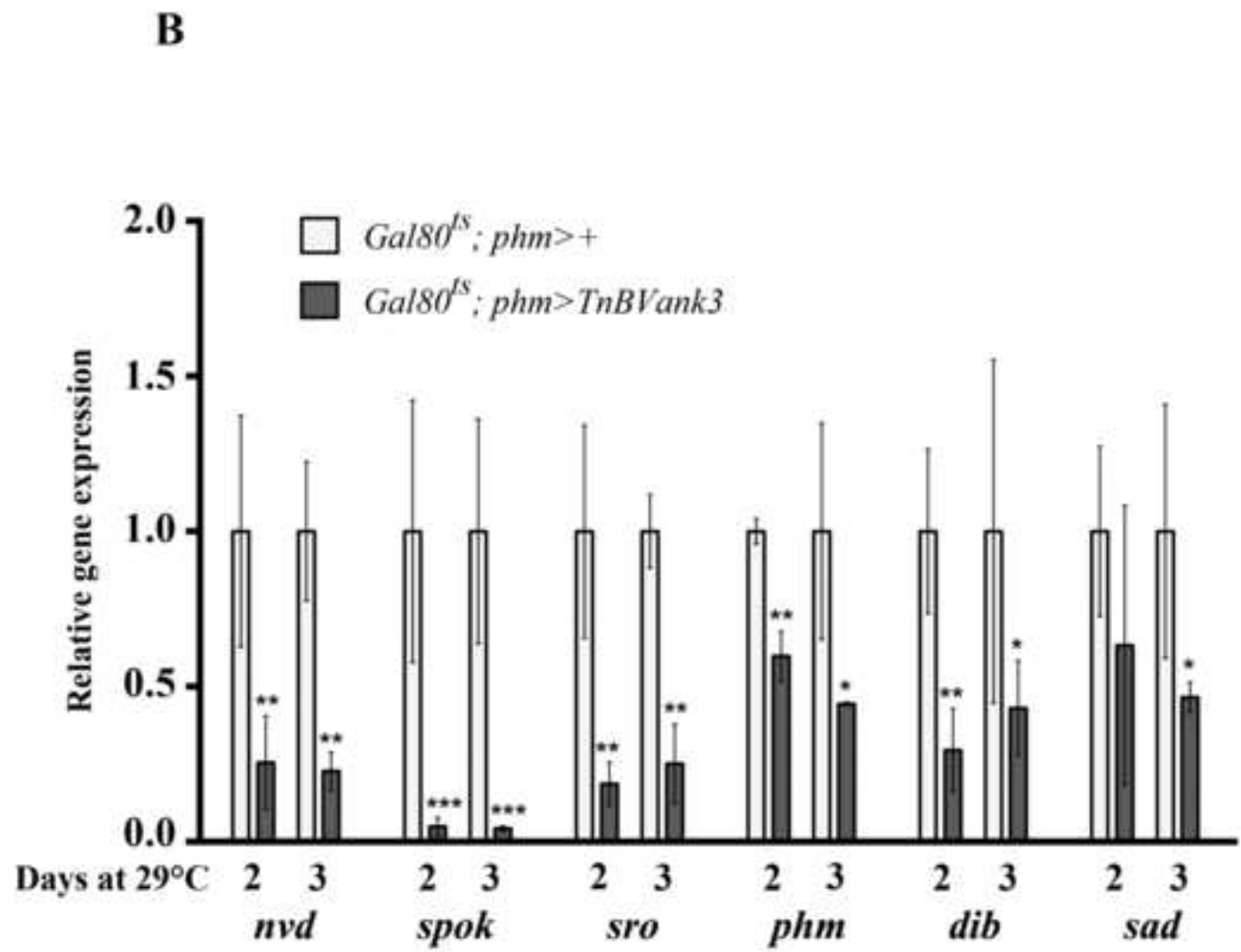
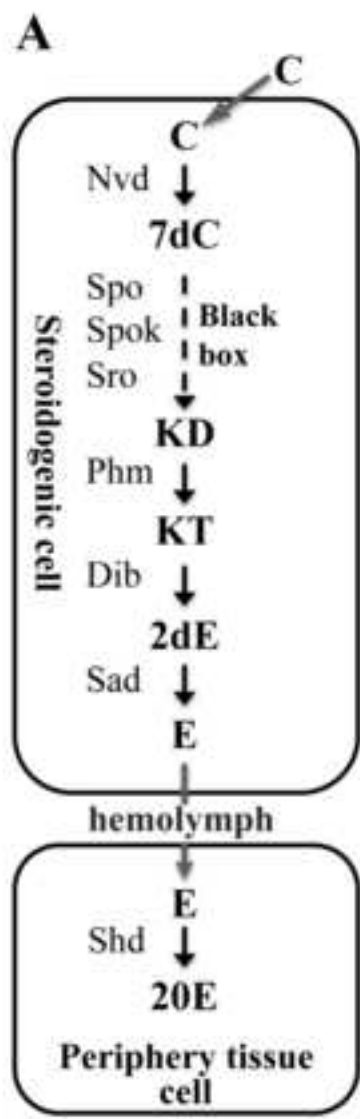


Figure 4

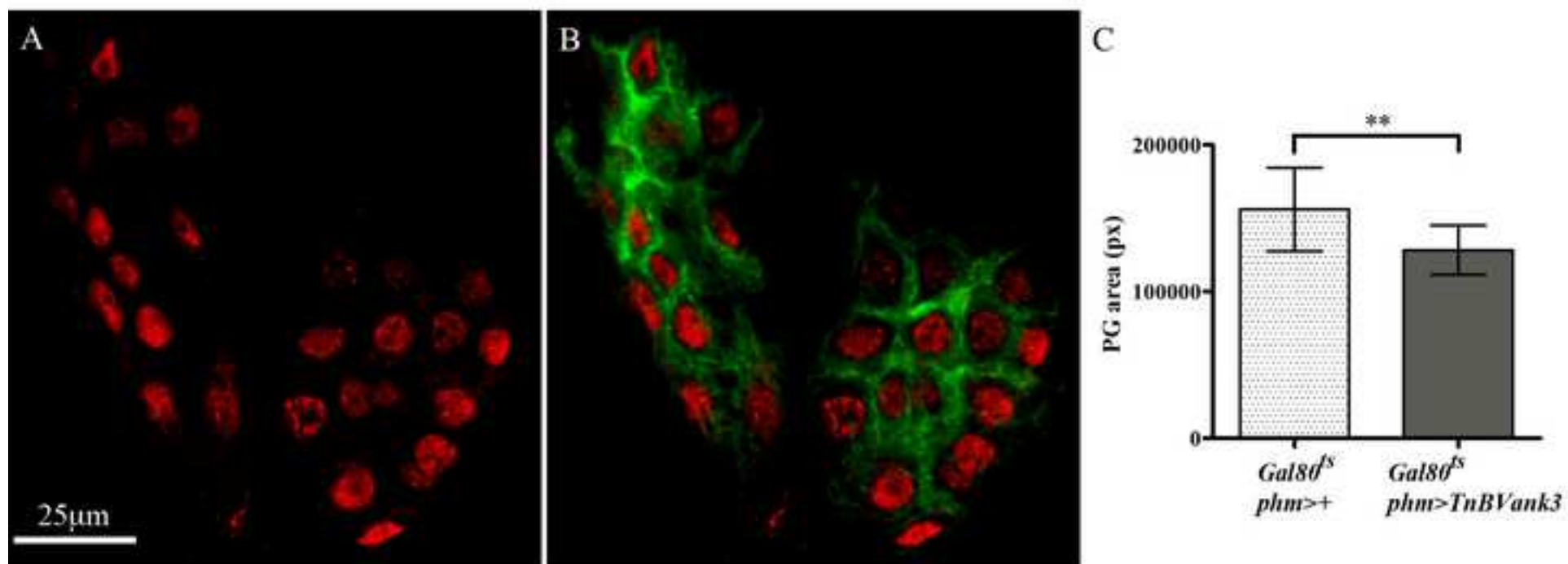
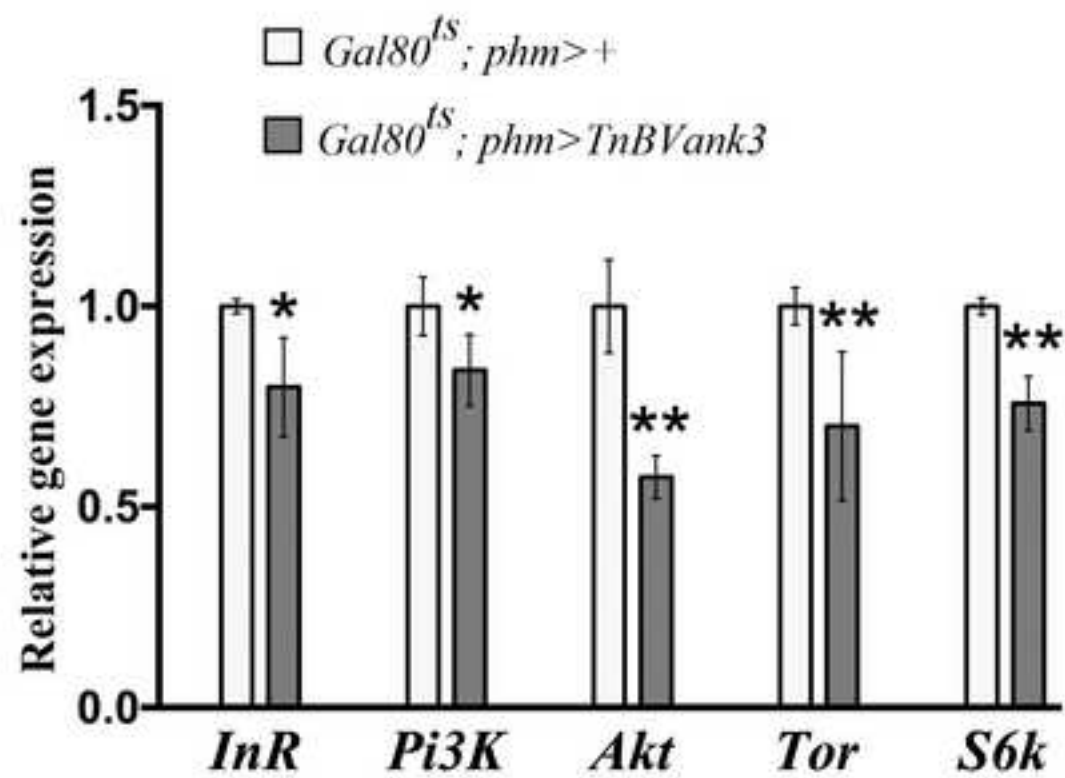


Figure 5

A



B

